

Two-photon excited hemoglobin fluorescence

Wei Zheng,^{1,†} Dong Li,^{1,†} Yan Zeng,¹ Yi Luo,² and Jianan Y. Qu^{1,*}

¹Biomedical Engineering Program, Department of Electronic and Computer Engineering, Hong Kong University of Science and Technology, Hong Kong, China

²Bio-X Division, Hefei National Laboratory for Physical Science at the Microscale, University of Science and Technology of China, Hefei, Anhui 230026, China

[†]These authors contributed equally to this work

*eequ@ust.hk

Abstract: We discovered that hemoglobin emits high energy Soret fluorescence when two-photon excited by the visible femtosecond light sources. The unique spectral and temporal characteristics of hemoglobin fluorescence were measured by using a time-resolved spectroscopic detection system. The high energy Soret fluorescence of hemoglobin shows the spectral peak at 438 nm with extremely short lifetime. This discovery enables two-photon excitation fluorescence microscopy to become a potentially powerful tool for *in vivo* label-free imaging of blood cells and vessels.

©2010 Optical Society of America

OCIS codes: (170.0170) Medical optics and biotechnology; (300.6500) spectroscopy, time-resolved; (300.6410) Spectroscopy, multiphoton; (170.2520) Fluorescence microscopy; (180.4315) Nonlinear microscopy.

References

1. W. Denk, J. H. Strickler, and W. W. Webb, "Two-photon laser scanning fluorescence microscopy," *Science* **248**(4951), 73–76 (1990).
2. B. R. Masters, and P. T. C. So, *Handbook of Biomedical Nonlinear Optical Microscopy* (Oxford University Press, 2008).
3. W. R. Zipfel, R. M. Williams, R. Christie, A. Y. Nikitin, B. T. Hyman, and W. W. Webb, "Live tissue intrinsic emission microscopy using multiphoton-excited native fluorescence and second harmonic generation," *Proc. Natl. Acad. Sci. U.S.A.* **100**(12), 7075–7080 (2003).
4. D. Kleinfeld, P. P. Mitra, F. Helmchen, and W. Denk, "Fluctuations and stimulus-induced changes in blood flow observed in individual capillaries in layers 2 through 4 of rat neocortex," *Proc. Natl. Acad. Sci. U.S.A.* **95**(26), 15741–15746 (1998).
5. R. Jimenez, and F. E. Romesberg, "Excited state dynamics and heterogeneity of folded and unfolded states of cytochrome c," *J. Phys. Chem. B* **106**(35), 9172–9180 (2002).
6. W. Min, S. Lu, S. Chong, R. Roy, G. R. Holtom, and X. S. Xie, "Imaging chromophores with undetectable fluorescence by stimulated emission microscopy," *Nature* **461**(7267), 1105–1109 (2009).
7. D. Fu, T. Ye, T. E. Matthews, B. J. Chen, G. Yurtserver, and W. S. Warren, "High-resolution *in vivo* imaging of blood vessels without labeling," *Opt. Lett.* **32**(18), 2641–2643 (2007).
8. C. Zhang, K. Maslov, and L. V. Wang, "Subwavelength-resolution label-free photoacoustic microscopy of optical absorption *in vivo*," *Opt. Lett.* **35**(19), 3195–3197 (2010).
9. M. Weissbluth, *Hemoglobin: Cooperativity and Electronic Properties* (Springer-Verlag, New York, 1974).
10. Y. Kurabayashi, K. Kikuchi, H. Kokubun, Y. Kaizu, and H. Kobayashi, "S₂ → S₀ fluorescence of some metallotetraphenylporphyrins," *J. Phys. Chem.* **88**(7), 1308–1310 (1984).
11. H. Yu, J. S. Baskin, and A. H. Zewail, "Ultrafast dynamics of porphyrins in the condensed phase: II. Zinc tetraphenylporphyrin," *J. Phys. Chem. A* **106**(42), 9845–9854 (2002).
12. D. Li, W. Zheng, and J. Y. Qu, "Two-photon autofluorescence microscopy of multicolor excitation," *Opt. Lett.* **34**(2), 202–204 (2009).
13. D. Li, W. Zheng, and J. Y. Qu, "Imaging of epithelial tissue *in vivo* based on excitation of multiple endogenous nonlinear optical signals," *Opt. Lett.* **34**(18), 2853–2855 (2009).
14. K. M. Hilligsøe, T. V. Andersen, H. N. Paulsen, C. K. Nielsen, K. Mølmer, S. Keiding, R. Kristiansen, K. P. Hansen, and J. J. Larsen, "Supercontinuum generation in a photonic crystal fiber with two zero dispersion wavelengths," *Opt. Express* **12**(6), 1045–1054 (2004).
15. A. Mansouri, and A. A. Lurie, "Methemoglobinemia," *Am. J. Hematol.* **42**(1), 7–12 (1993).
16. S. F. Russo, and R. B. Sorstokke, "Hemoglobin. Isolation and chemical properties," *J. Chem. Educ.* **50**(5), 347–350 (1973).
17. E. J. van Kampen, and W. G. Zijlstra, "Determination of hemoglobin and its derivatives," in *Advances in Clinical Chemistry*, H. Sobotka and C. P. Stewart, eds. (Academic, 1965), pp. 158–187.
18. O. W. van Assendelft, *Spectrophotometry of Haemoglobin Derivatives* (Royal Vangorcum, 1970).

19. Y. Mendelson, and J. C. Kent, "Variations in optical absorption spectra of adult and fetal hemoglobins and its effect on pulse oximetry," *IEEE Trans. Biomed. Eng.* **36**(8), 844–848 (1989).
 20. P. T. C. So, C. Y. Dong, B. R. Masters, and K. M. Berland, "Two-photon excitation fluorescence microscopy," *Annu. Rev. Biomed. Eng.* **2**(1), 399–429 (2000).
 21. A. Diaspro, G. Chirico, and M. Collini, "Two-photon fluorescence excitation and related techniques in biological microscopy," *Q. Rev. Biophys.* **38**(2), 97–166 (2005).
 22. C. C. Winterbourn, "Free-radical production and oxidative reactions of hemoglobin," *Environ. Health Perspect.* **64**, 321–330 (1985).
 23. J. Balaji, C. S. Reddy, S. K. Kaushalya, and S. Maiti, "Microfluorometric detection of catecholamines with multiphoton-excited fluorescence," *Appl. Opt.* **43**(12), 2412–2417 (2004).
 24. C. Li, R. K. Pastila, C. Pitsillides, J. M. Runnels, M. Puoris'haag, D. Côté, and C. P. Lin, "Imaging leukocyte trafficking in vivo with two-photon-excited endogenous tryptophan fluorescence," *Opt. Express* **18**(2), 988–999 (2010).
 25. E. N. Marieb, *Essentials of Human Anatomy & Physiology*, 9th ed. (Benjamin Cummings, 2008).
-

1. Introduction

Two-photon excitation fluorescence (TPEF) microscopy has become a mainstream biological imaging tool after two decades of development [1–3]. In particular, noninvasive label-free imaging capability of TPEF microscopy can be achieved by using the fluorescence emission from the endogenous fluorescent molecules in living cells and tissue, such as the reduced nicotinamide adenine dinucleotide (NADH), tryptophan, flavin adenine dinucleotide (FAD), keratin, collagen and elastin etc. These endogenous fluorescence signals provide rich morphologic and biochemical information of the imaged biological samples. However, TPEF microscopy has to rely on exogenous fluorescent agents for three dimensional (3-D) volumetric visualization of the delicate features of microvasculature and the contrast agents could induce disturbance to the biological processes in the living cells and tissue [4]. The difficulties for label-free visualizing of blood is associated with the widely spread hypothesis that hemoglobin has undetectable fluorescence due to that its spontaneous emission is dominated by the fast non-radiative decay of the excited states [5,6]. The current techniques for imaging of blood cells and vessels are mainly based on the absorption of hemoglobin, the major component of blood. For example, recently developed stimulated emission microscopy and excited state absorption took the advantage of large absorption coefficient of hemoglobin and permit label-free imaging of erythrocytes (red blood cells) with high sensitivity and resolution [6,7]. The pump-probe imaging methods require sophisticated excitation sources. The signals of stimulated emission or excited state absorption could be interfered by other chromophores of absorption spectra overlapping with hemoglobin. A subwavelength-resolution photoacoustic microscopy for *in vivo* vasculature imaging was demonstrated very recently [8]. The technique is also based on the absorption of hemoglobin.

It is well known that hemoglobin, like other metalloporphyrins, possesses two well separated absorption states, named as Q-band and Soret band (or B-band) as shown in Fig. 1, respectively [9]. Certain type of metalloporphyrins can emit fluorescence from both states centered normally at 650 nm and 430 nm, respectively [10], owing to the large energy separation between them. In particular, the unique high energy emission from the Soret band can become detectable when it is not quenched by inter- and intra-molecular interactions [11]. Indeed, we discovered for the first time that hemoglobin emits blue TPEF signal when it is excited by the visible femtosecond laser light. In this work, we first characterize the TPEF signals measured from the hemoglobin solutions in time and wavelength domains. Then we verify that the fluorescence signals emitted from the erythrocytes originate from the hemoglobin and demonstrate that hemoglobin fluorescence can provide good contrast to image the erythrocytes. In principle, this implementation could be easily incorporated into a standard mainstream two-photon excitation microscopy for noninvasive imaging of erythrocytes and microvasculature *in vivo*.

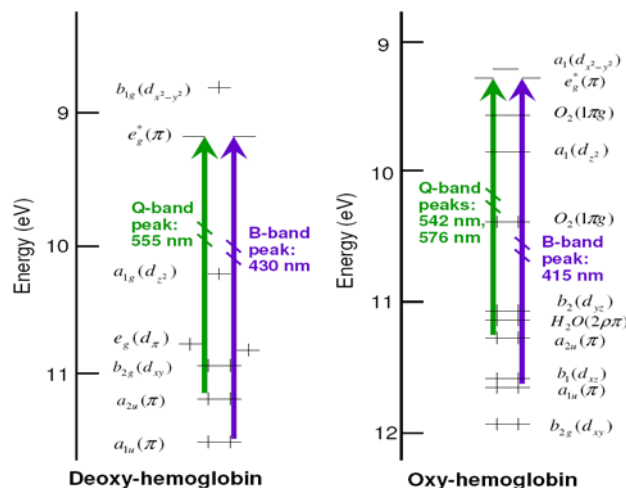


Fig. 1. The electronic energy level diagram of hemoglobin (The Soret or B- and Q-bands are due to transitions between the $a(\pi)$ and $e_g(\pi)$ orbitals).

2. Methods and Materials

2.1 Instrumentation of time-resolved spectroscopic imaging system

A time-resolved spectroscopic imaging system (Fig. 2) was instrumented for the study of two photon excited Soret fluorescence of hemoglobin [12,13]. The excitation sources in the wavelength range of 600-750 nm were from a tunable femtosecond Ti:sapphire laser and the ultrafast supercontinuum generation in a photonic crystal fiber. A long pass filter (HQ680LP, Chroma) was placed at the exit of the femtosecond laser to remove the superfluorescence from the laser. The supercontinuum was generated from a photonic crystal fiber (PCF, NL-1.4-775, Crystal Fiber). The femtosecond Ti:sapphire laser (Mira 900, Coherent) of wavelength tuned at 745 nm was used as the pump source [14]. The supercontinuum beam in visible band was purified by an interference band-pass filters at 600 ± 20 nm (D600/40M, Chroma) or 650 ± 22 nm (HQ650/45X, Chroma) to produce the femtosecond excitations of wavelength below 700 nm. In the study of hemoglobin fluorescence excited at the wavelength over 700 nm, the tunable laser light was used as the excitation source directly. The full width at half maximum (FWHM) of the autocorrelation curves for the supercontinuum at 600 nm and 650 nm and the Ti:sapphire laser light measured by an autocorrelator (Pulsecheck-50, APE GmbH, Germany) were about 800 fs, 600 fs and 250 fs, respectively. The excitation power of each beam was less than 15 mW on the sample. A water immersion objective ($40 \times$, 1.15 NA, Olympus) was used to focus the excitation beam(s) into the examined samples and collect the backscattered TPEF signals. A sampling area, typically 50×50 μm or 100×100 μm , was created by scanning a pair of x-y galvo mirrors. The objective lens was driven by an actuator to achieve the depth scanning. A dichroic mirror (FF510, Semrock) was placed above the objective to reflect the TPEF signals to the detection system and a short-pass filter (SP01-532RU or FF01-680/SP, Semrock) was used to reject the reflected excitation light. The TPEF signals were relayed by a telescope to a fiber bundle that conducted the TPEF signals to a spectrograph. For the spectroscopic measurements of hemoglobin solutions, a cooled CCD (NTE/CCD-1340/400-EMB, Roper Scientific, Trenton, New Jersey) was used to record high-resolution TPEF spectra in the range from 400 to 530 nm. For the TPEF lifetime measurement and spectroscopic imaging, the CCD detector was replaced with a linear array of photomultiplier tubes (PMT) connected with a time-correlated single photon counting (TCSPC) module (PML-16-C-0 and SPC-150, Becker & Hickl). The system recorded time-resolved fluorescence signals in 16 consecutive spectral bands from 300 to 500 nm at 13 nm interval and provided the capability to simultaneously detect TPEF signal in time and

wavelength domains. The microscope imaging system produced lateral and axial resolutions of about 0.4 and 1.5 μm , respectively. The spectrum and image acquisition time was set to 8 seconds.

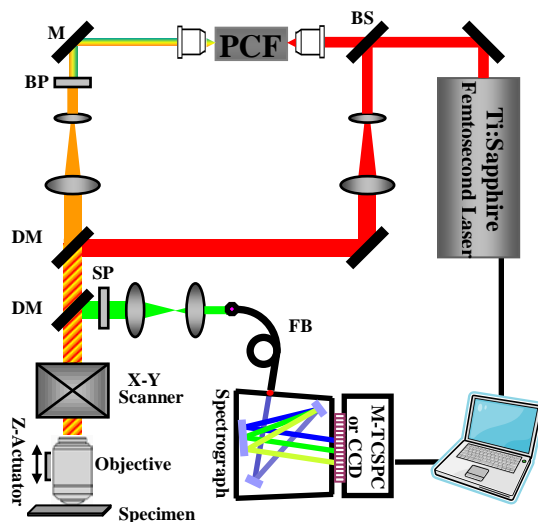


Fig. 2. Schematic diagram of the spectroscopic imaging system. BS: beam splitter; M: mirror; BP: band-pass filter; DM: dichroic mirror; SP: short-pass filter; FB: fiber bundle; M-TCSPC: time-correlated single photon counting (TCSPC) module equipped with a multichannel PMT array.

2.2 Chemical solution preparation

The stabilized human lyophilized ferrous hemoglobin powder (H0267) was purchased from Sigma-Aldrich for the preparation of hemoglobin solutions. According to the product information, the highly purified hemoglobin powder was obtained via standard chromatographic separation method. However, the powders consist of certain amount of ferric hemoglobin (<15%) that were produced during the processes of purification and packaging (see description of Sigma-Aldrich hemoglobin products at <http://www.sigmaaldrich.com/life-science/biochemicals/biochemical-products.html?TablePage=16192492>). This indicated that the signal measured from the solutions made of Sigma hemoglobin powder would be a mixture of ferrous and ferric hemoglobin. To study the interference from the ferric hemoglobin (methemoglobin), we prepared the solutions for the TPEF spectroscopy measurements using the pure methemoglobin powder (M5882) purchased from Sigma-Aldrich.

It is well known that the native hemoglobin in blood is dominated by ferrous hemoglobin [15]. The measurement of the TPEF signal from the ferrous hemoglobin solution is desirable for this study. In order to reduce the oxidization of hemoglobin and avoid the interference of methemoglobin, we extracted the hemoglobin from fresh blood sample following a simple standard procedure [16]. Because of the existence of the methemoglobin reductase in the fresh blood [15], it is expected that the home-extracted hemoglobin sample is dominated by ferrous hemoglobin. In the extraction of hemoglobin, the blood cells in the blood sample freshly withdrawn from mice were packed by spinning at 3000 rpm for 3 minutes and then washed with phosphate buffered saline (PBS) to remove the plasma. This procedure was repeated for a few times to ensure that the plasma was completely removed. Then one unit volume of blood cells was thoroughly mixed with one unit volume of deionized water and 0.4 volume of toluene. The mixture was stored at 4°C for at least 24 hours to ensure complete hemolysis. The solution was then spun at 13000 rpm for 10 minutes and the layer of clear hemoglobin solution was aspirated by using a syringe. This solution was then filtered by using a syringe

filter (Millex, Millipore) with pore size of 0.22 μm to remove the cell debris, particles and large molecules. The filtered hemoglobin solution was stored at 4°C for future use. We found that the absorption spectrum of extracted hemoglobin was identical to the oxyhemoglobin. The hemoglobin concentration in the solution was then determined by the oxyhemoglobin absorption spectrum with a commercial absorption spectrometry (Ultraspec 4300 pro UV/Visible Spectrophotometer, GE Healthcare, UK) [17,18].

In this work, we studied the TPEF characteristics of the solutions made of Sigma hemoglobin, Sigma methemoglobin and home-extracted hemoglobin of concentrations about 15g/L, 20g/L and 50g/L, respectively. The solutions were held in a cuvette with a microscope coverslip as the TPEF measurement window. To prevent the possible strong hemoglobin re-absorption to the TPEF signal, we kept the focal point of excitation at about 5 μm below the coverslip to make sure that the measured sample was optically thin. We found that the re-absorption to the fluorescence was negligible because the TPEF spectral characteristics remained unchanged by further diluting the hemoglobin samples. To study the TPEF signals from oxygenated and deoxygenated blood, the oxyhemoglobin was prepared by saturation of the hemoglobin solution with the oxygen gas, and the deoxyhemoglobin was derived by adding sodium dithionite to the hemoglobin solution. The absorption spectra of oxyhemoglobin and deoxyhemoglobin solutions were measured by using a commercial absorption spectrometry to precisely determine the oxygen saturation in the oxyhemoglobin and deoxyhemoglobin solutions, respectively [19].

2.3 Estimation of relative two-photon excitation efficiency

For femtosecond laser with wavelength λ_{ex} , pulse repetition rate f_p , pulse width τ_p , and average power P_{ave} , the collectable TPEF intensity is given by following relationship [20,21]:

$$I_f = \kappa\pi\delta_2\eta \frac{P_{ave}^2}{\tau_p f_p} \left(\frac{(NA)^2}{hc\lambda_{ex}} \right)^2 \quad (1)$$

where κ and NA are a factor taking into account the collection efficiency and the numerical aperture of the microscope system, respectively. h and c are the Planck's constant and speed of light, respectively. Therefore, for the measurements of a sample with the same imaging setup, the relative excitation efficiency of the TPEF signal at different excitation wavelengths, $\eta_2(\lambda_{ex})$, can be estimated as:

$$\eta_2(\lambda_{ex}) = \varepsilon \frac{I_f \tau_p \lambda_{ex}^2}{P_{ave}^2} \quad (2)$$

where ε is a proportional constant, while I_f , τ_p and P_{ave} are three measurables. In this study, I_f is the fluorescence signal detected by the cooled CCD. The pulse width τ_p and the averaged excitation power P_{ave} of supercontinuum and laser at different wavelengths were measured using an autocorrelator (Pulsecheck-50, APE GmbH, Germany) and a power meter (Model 2832-C Dual-channel power meter, Newport, USA), respectively. It should be pointed out that since the excitation light at 600 and 650 nm are filtered out from the supercontinuum. Their pulse shapes are different from the nearly transform limited Gaussian pulse of the Ti:Sapphire femtosecond laser. This may cause certain error in the comparison of the excitation efficiency of supercontinuum pulses at 600 nm and 650 nm with the laser pulses of wavelength over 700 nm.

3. Results and discussions

3.1 TPEF characteristics of the chemical solutions

We measured the TPEF spectra of Sigma hemoglobin solution excited by the femtosecond light of wavelength range from 600 to 750 nm. As shown in Fig. 3(a), although the spectral peaks of hemoglobin remain around 440 nm at different excitation wavelengths, the shoulder

in long wavelength region is clearly elevated with the increase of excitation wavelength. As indicated previously, the hemoglobin powder from Sigma-Aldrich contains ~15% methemoglobin. The measured TPEF spectra must be the mixture of hemoglobin and methemoglobin signals. To study whether the signal of methemoglobin, the major interference composition in the hemoglobin powder, could distort the TPEF spectral characteristics of hemoglobin, we measured the TPEF fluorescence spectra from the pure methemoglobin solution. The TPEF spectra of methemoglobin excited at different wavelengths are shown in Fig. 3(b). As can be seen, the spectral lineshapes of methemoglobin are completely different from those measured from Sigma hemoglobin solution as shown in Fig. 3(a). Furthermore, we calculated the excitation efficiency of TPEF signals from Sigma hemoglobin and methemoglobin. The results are presented in Fig. 3(c). We found that the fluorescence excitation efficiency of Sigma hemoglobin decreases rapidly with the increase of excitation wavelength, while the excitation efficiency of methemoglobin fluorescence does not change significantly. Therefore, the TPEF signals of Sigma hemoglobin excited at 600 nm should be dominated by the fluorescence of ferrous hemoglobin because of its higher excitation efficiency and concentration. However, the contribution of methemoglobin signal becomes significant at longer excitation wavelength. In addition, we studied the temporal characteristics of TPEF signals from the Sigma hemoglobin and methemoglobin solutions. The representative results excited at 600 nm are shown in Fig. 3(d). We found that the time-resolved fluorescence signals from both solutions are almost identical to the system response about 230 ps (FWHM), indicating the extremely short fluorescence lifetime. This may be due to the extremely short excited state lifetime of Soret band because of its strongly allowed transition and competition with fast intersystem crossing.

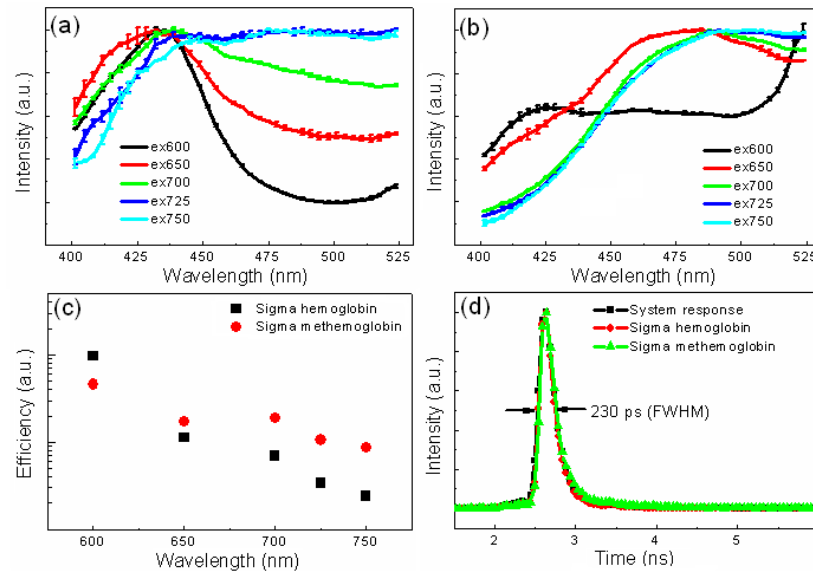


Fig. 3. TPEF characteristics of Sigma hemoglobin and methemoglobin. (a) TPEF spectra of hemoglobin (Sigma-Aldrich, H0267) excited at the wavelengths from 600 to 750 nm; (b) TPEF spectra of methemoglobin (Sigma-Aldrich, M5882); (c) Excitation efficiency of hemoglobin and methemoglobin as a function of excitation wavelength; (d) Time-resolved hemoglobin and methemoglobin two-photon fluorescence excited at 600 nm.

Next, we measured TPEF signals from the solution made of the home-extracted hemoglobin. In order to verify whether the home-extracted hemoglobin is dominated by ferrous hemoglobin, we compared the 600 nm excited TPEF spectrum acquired from home-extracted hemoglobin solution with that measured from Sigma hemoglobin solution. The results are shown in Fig. 4(a). As can be seen, two spectra mainly overlap with each other except at short and long wavelength edges. The inconsistency at edges may be contributed

from the methemoglobin in the Sigma hemoglobin sample. The close similarity between two spectra provides evidence that the ferrous hemoglobin is dominant in the home-extracted sample. Because the hemoglobin signal measured from the home-extracted solution would be less distorted by methemoglobin, we used the home-extracted solution to characterize the hemoglobin TPEF signals in the following study.

We measured the TPEF signals from home-extracted hemoglobin solutions excited by the femtosecond pulse light of wavelength range from 600 to 750 nm. Detailed TPEF characteristics are shown in Fig. 4(b-e). The fluorescence emission peak is located at about 438 nm when the excitation light is in the range from 600 nm to 750 nm as shown in Fig. 4(b). This is consistent with the Soret fluorescence emission wavelength of other metalloporphyrins reported previously [10]. We noticed that a constant background appeared in all the TPEF spectra measured from the hemoglobin solutions and the erythrocyte sample in following experiments. However, its origin has not been identified yet. The Soret band should have a very short lifetime because of its strongly allowed transition and competition with fast intersystem crossing. Again, this is partially confirmed by our measured fluorescence intensity decay shown in Fig. 4(c), which is almost identical to the system response about 230 ps (FWHM). As can be seen from Fig. 4(d), the hemoglobin fluorescence is effectively excited when the excitation wavelength is below 700 nm, which is simply due to the near resonance with the Q-band as indicated in the energy level diagram in Fig. 1. The fluorescence signal becomes very weak when the excitation wavelength is over 750 nm. This may explain why two-photon excited hemoglobin fluorescence was not observed previously. The measured fluorescence intensity shows a quadratic dependency on the excitation power as presented in the inset figure of Fig. 4(d), proving that the observed Soret fluorescence of hemoglobin is a result of two-photon excitation process. The fluorescence spectrum of oxyhemoglobin and deoxyhemoglobin are shown in Fig. 4(e). It is found that there are no significant difference in spectral characteristics between oxyhemoglobin and deoxyhemoglobin.

Furthermore, we measured the oxidation dependent TPEF signals to further verify that the measured two-photon fluorescence signal was indeed from ferrous hemoglobin. It is known that the oxidation of ferrous hemoglobin turns the iron atom from divalent to trivalent, resulting in ferric hemoglobin, named methemoglobin. A standard procedure was followed to oxidize the hemoglobin solution [22]. The TPEF spectra of the solution before and after oxidation by adding hydrogen peroxide are presented in Fig. 4(f), in which the spectrum of pure methemoglobin purchased from Sigma-Aldrich is presented for a comparison. It can be clearly seen that the oxidized hemoglobin has produced almost identical spectrum as the pure methemoglobin. With all these evidences, we can firmly conclude that the origin of the observed fluorescence emission peaked at 438 nm is indeed hemoglobin.

Finally, we compared the two-photon excitation cross-section of hemoglobin with that of tryptophan at 600 nm excitation because the two-photon excitation cross-section of tryptophan has been studied [23]. In addition, the tryptophan fluorescence has been demonstrated to produce high contrast images from living animal model *in vivo* [13,24]. It could be used to predict whether the hemoglobin fluorescence is detectable at tissue level. In this study, the tryptophan (T0254, Sigma) was dissolved at the concentration of 5 mM in deionized water. The concentration of the hemoglobin solution was precisely measured by a standard method based on the absorption spectra [17,18]. All solutions were adjusted to about pH 7.0. We measured the TPEF signals from the hemoglobin and tryptophan solutions under the same excitation condition. The detection system was the 16-channel PMT array with response calibration from 300 to 500 nm, covering the TPEF signals of tryptophan and hemoglobin. The comparison results show that the two-photon excitation cross-section of hemoglobin is about a factor of 3 higher than that of tryptophan.

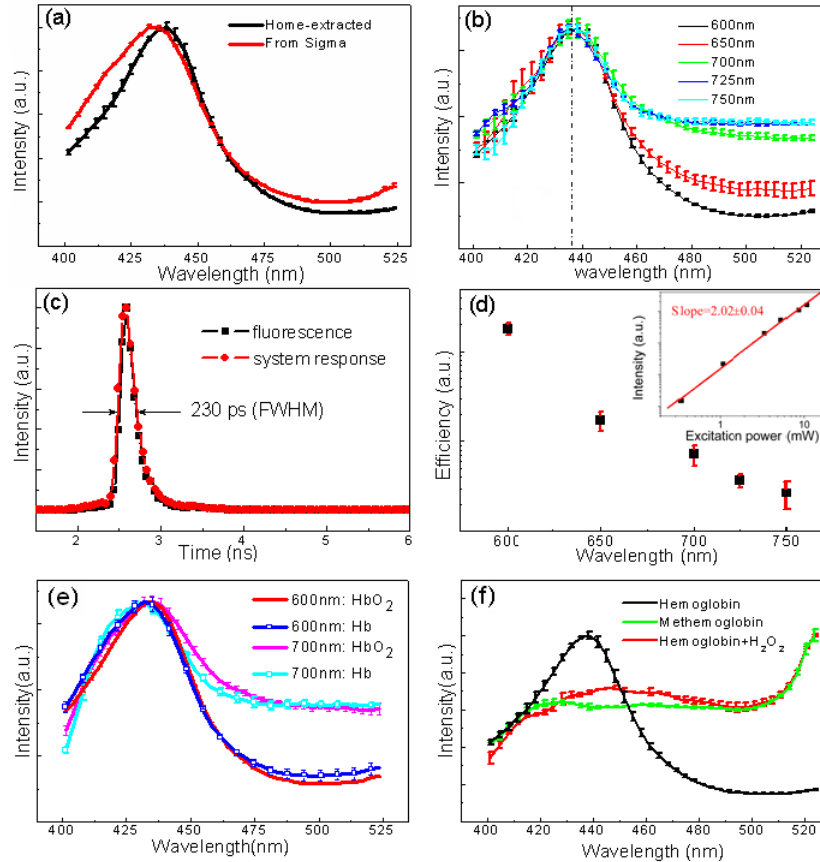


Fig. 4. Spectral and temporal TPEF characteristics of home-extracted hemoglobin. (a) TPEF spectrum of Sigma and home-extracted hemoglobin excited at 600 nm; (b) TPEF spectra of home-extracted hemoglobin excited at different wavelengths; (c) Time decay curve of the fluorescence excited at 600 nm; (d) Excitation efficiency as a function of excitation wavelength. Inset: dependency of fluorescence signal on excitation power; (e) TPEF spectra of oxy- and deoxy-hemoglobin excited at 600 nm and 700 nm; (f) TPEF spectra of methemoglobin and hemoglobin before and after oxidation by using hydrogen peroxide.

3.2 TPEF images and characteristics of erythrocytes

Hemoglobin is the dominant component in erythrocytes (red blood cells) that constitute about 45% of whole blood by volume, while the plasma constitute about 54.3% and leukocytes (white blood cells) about only 0.7% [25]. Here, we explored the potential of imaging erythrocytes based on the intrinsic hemoglobin fluorescence. We focused on the hemoglobin fluorescence excited at 600 nm because of its high excitation efficiency. Moreover, the spectral and temporal characteristics of TPEF signals from blood cells were recorded by the time-resolved spectroscopic imaging system that analyzed the signals in both time and wavelength domains [12,13]. A TPEF image of the erythrocytes sample freshly extracted from mice blood is shown in Fig. 5(a), from which the individual doughnut-shaped erythrocytes are clearly visualized. The image was formed using the TPEF signal in the wavelength band of 420-460 nm, covering the peak of hemoglobin Soret fluorescence. To analyze the characteristics of the fluorescence from erythrocytes, we integrated the signals recorded at all pixels of erythrocytes to produce the TPEF spectrum and time-decay of erythrocytes fluorescence, respectively. As shown in Fig. 5(b), the spectral and temporal characteristics of erythrocytes TPEF signals are almost the same as those measured from

hemoglobin solution. The results demonstrated that the fluorescence signals used to form the image of erythrocytes were indeed originated from hemoglobin in the cells.

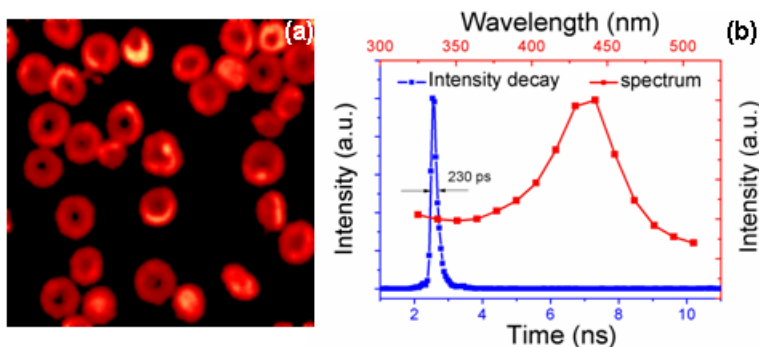


Fig. 5. Image and fluorescence characteristics of erythrocytes at 600 nm excitation. (a) TPEF image of erythrocytes in PBS solution (The sampling area of the image: $50 \times 50 \mu\text{m}$); (b) TPEF spectrum and time decay curve of erythrocytes.

4. Conclusion

In summary, we discovered Soret fluorescence emission from hemoglobin via two-photon excitation. The spectral and lifetime characteristics of the hemoglobin and methemoglobin fluorescence have been studied by using a time-resolved spectroscopic imaging system. The hemoglobin fluorescence provides sharp contrast to image individual erythrocyte. Because of the relatively large two-photon excitation cross-section of hemoglobin, the TPEF fluorescence could be used for label-free imaging the microvasculature from heterogeneous tissue constituents based on its unique spectral and temporal characteristics of hemoglobin fluorescence.

Acknowledgments

We acknowledge support from the General Research Fund of Hong Kong Research Grant Council (Grant No. 618808) and Hong Kong University of Science and Technology (Grant RPC10EG33).